

Individualized Multi-Treatment Response Curves Estimation using RBF-net with Shared Neurons

PETER CHANG, ARKAPRAVA ROY

Department of Biostatistics, University of Florida, United States

pchang27@ufl.edu, arkaprava.roy@ufl.edu

October 21, 2024

Abstract

Heterogeneous treatment effect estimation is an important problem in precision medicine. Specific interests lie in identifying the differential effect of different treatments based on some external covariates. We propose a novel non-parametric treatment effect estimation method in a multi-treatment setting. Our non-parametric modeling of the response curves relies on radial basis function (RBF)-nets with shared hidden neurons. Our model thus facilitates modeling commonality among the treatment outcomes. The estimation and inference schemes are developed under a Bayesian framework using thresholded best linear projections and implemented via an efficient Markov chain Monte Carlo algorithm, appropriately accommodating uncertainty in all aspects of the analysis. The numerical performance of the method is demonstrated through simulation experiments. Applying our proposed method to MIMIC data, we obtain several interesting findings related to the impact of different treatment strategies on the length of ICU stay and 12-hour SOFA score for sepsis patients who are home-discharged.

Keywords: Bayesian; ICU; MIMIC data; Multi-treatment regime; Radial basis network; Treatment effect.

1 Introduction

In many clinical settings, such as intensive care units (ICUs), patients often receive multiple treatments simultaneously. For instance, in the MIMIC database, septic patients frequently receive both mechanical ventilation and vasopressors, either separately or simultaneously (Peine et al., 2021; Zhu et al., 2021; Xu et al., 2023; He et al., 2023). Similarly, in clinical trials, treatment arms often share a common drug across different interventions (James et al., 2016; Ursprung et al., 2021), reflecting potential commonalities in treatment effects. Recognizing that treatments may share underlying mechanisms, which influence the outcomes (Jones et al., 2003; White et al., 2011), it becomes important to adequately account for these shared characteristics in the model. This motivates the development of the proposed model to estimate heterogeneous treatment effects with shared characteristics.

Estimating heterogeneous treatment effects from observational data is crucial for determining individualized causal effects (Wendling et al., 2018) and learning optimal personalized treatment assignments (Rekkas et al., 2020; Zhang et al., 2012; Jiang et al., 2017; Cui and Tchetgen Tchetgen, 2021; Li, Chen, Laber, Liu and Baumgartner, 2023). However, accurate estimation requires reasonable representations from each treatment subgroup. The advent of large-scale health outcome data, such as electronic health records (EHRs), has significantly optimized the design of several novel statistical methods, primarily tailored for binary treatment scenarios (Wendling et al., 2018; Cheng et al., 2020), with some accommodating multiple treatment settings (Brown et al., 2020; Chalkou et al., 2021). While many approaches focus on estimating population average treatment effects (ATEs) (Van Der Laan and Rubin, 2006; Chernozhukov et al., 2018; McCaffrey et al., 2013), newer methods aim to estimate conditional average treatment effects (CATEs) (Taddy et al., 2016; Wager and Athey, 2018; Künzel et al., 2019).

In a binary setting, the treatment effect $\tau(\mathbf{x})$ can be estimated as a function of the predictor vector \mathbf{x} with a mean-zero additive error model. Here, the continuous treatment outcome y_i is expressed as $y_i = f(\mathbf{x}_i, z_i) + \epsilon_i$, where z_i is a treatment indicator for the i -th subject. Under this model, $\tau(\mathbf{x}_i) = f(\mathbf{x}_i, 1) - f(\mathbf{x}_i, 0)$. Another possibility $f(\mathbf{x}_i, z_i) = \mu(\mathbf{x}_i) + \tau(\mathbf{x}_i)z_i$ (Hahn et al., 2020) can also be used for a direct estimation of the treatment effect. Alternatively, one may model each treatment group separately with two functions $f_0(\mathbf{x}_i)$ and $f_1(\mathbf{x}_i)$ and define $\tau(\mathbf{x}_i) = f_1(\mathbf{x}_i) - f_0(\mathbf{x}_i)$.

These two approaches are defined as S-learner and T-learner, respectively (Künzel et al., 2019). On Bayesian causal inference, Li, Ding and Mealli (2023) provides a critical review. In a multi-treatment setting, one may either develop a model with the treatment indicator as a predictor as in S-learning or set treatment-specific functions as in T-learning. However, traditional T-learners do not work very well when a common behavior is expected in two response functions, as shown in Künzel et al. (2019) for a two-treatment design.

To address these limitations, we propose a radial basis function-based modeling approach that accommodates shared characteristics between outcomes and captures both shared and treatment-specific features. Our model allows the recognition of treatments sharing common underlying pathways or characteristics, thus improving the accuracy of treatment effect estimates. Here, we tackle a generic problem of heterogeneous treatment effect or CATE estimation in a multi-treatment setting, where the treatment responses may share some commonalities. The proposed model can be applied in estimating outcome functions, particularly when they are expected to share common characteristics.

We further propose a thresholding-based inference procedure relying on the best linear projections from Cui et al. (2023). Specifically, we first modify the approach from Cui et al. (2023) for inference using the posterior samples and then propose a variable importance estimation procedure by combining a thresholding step. The estimated importance values are shown to work reasonably well in simulation and are later used for inference in our MIMIC application.

The remainder of this article is organized as follows. The subsequent section introduces our proposed modeling framework. Section 3 discusses our Bayesian inference scheme detailing the prior specification, likelihood computation, detailed posterior computation steps, and linear projection-based inference scheme. Subsequently, in Section 4, we analyze and compare the effectiveness of our proposed method against other competing approaches under various simulation settings. Finally, we apply our proposed method to study the effect of different treatments on patients, who suffered from acute sepsis and were discharged to home at the end of their ICU visit using MIMIC data in Section 5, and Section 6 is dedicated to discussing the overall conclusion and potential extensions.

2 Model

Our proposed model falls under the class of T-learner type models. We consider G treatments and assume that there are P covariates. Let y_i be a continuous treatment outcome for the i -th patient with subject-specific P -dimensional covariates specified by \mathbf{x}_i . Then, our model for y_i when treated under the g -th treatment is,

$$y_i = f_g(\mathbf{x}_i) + \epsilon_i, \quad (1)$$

$$\epsilon_i \sim \text{Normal}(0, \sigma^2), \quad (2)$$

$$f_g(\mathbf{x}_i) = \alpha + \sum_{k=1}^K \gamma_{k,g} \theta_k \exp\{-(\mathbf{x}_i - \boldsymbol{\mu}_k)^T (\mathbf{x}_i - \boldsymbol{\mu}_k) / b_k^2\}. \quad (3)$$

Here, $f_1(\cdot), \dots, f_G(\cdot)$ denote the treatment-specific outcome functions modeled using a common set of radial basis function (RBF) neurons. Each function has a treatment-specific parameter $\boldsymbol{\gamma}_g = (\gamma_{k,g})_{1 \leq k \leq K}$ in its coefficients, where $\gamma_{k,g} \in \{0, 1\}$, and $\boldsymbol{\mu}_k, \theta_k \in \mathbb{R}$. We then construct the parameter $\boldsymbol{\Gamma} = ((\gamma_{k,g}))_{1 \leq k \leq K, 1 \leq g \leq G}$ as a $K \times G$ dimensional binary matrix. This matrix plays a crucial role in our proposed model, controlling the set of RBF bases to be used in specifying a treatment-specific outcome function. Here, $\gamma_{k,g}$ is 1 whenever the k -th RBF basis is included in modeling $f_g(\mathbf{x})$. A schematic representation of the proposed mode is in Figure 1. Note that the flexibility of the proposed model automatically extends to the cases with minimal to no sharing among the f_g 's.

The role of $\boldsymbol{\Gamma}$ is to address the inefficiency mentioned previously about T-learner type models. Though $\boldsymbol{\Gamma}$ determines the shared and treatment-specific RBF bases, its primary role is to improve the estimation of outcome functions that may share common characteristics, rather than explicitly identifying similarities and differences between responses.

In our proposed model, the conditional treatment effect of g over g' for an array of covariates \mathbf{x} is identified as $\tau_{gg'} = f_g(\mathbf{x}) - f_{g'}(\mathbf{x})$ under assumptions that 1) given \mathbf{x} , treatment assignments are random and do not depend on the outcome, 2) the overlap condition $1 > P(z_i = g \mid \mathbf{x}_i) > 0$ holds for all i , where z_i is the treatment assignment variable such that $z_i = g$ implies i -th subject is treated under g -th treatment and 3) standard stable unit treatment value assumption (SUTVA) is maintained requiring no interference that one subject's potential outcomes are not affected by

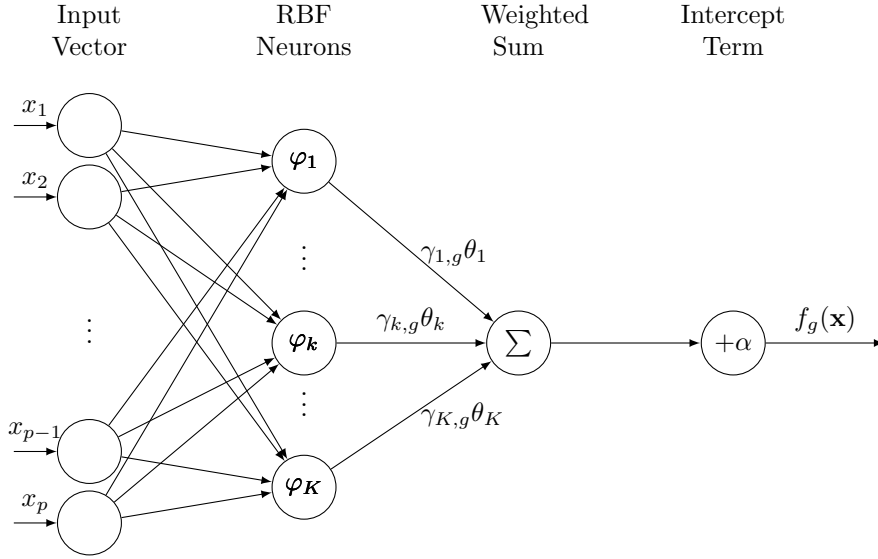


Figure 1: A schematic representation of our proposed RBF-net where $\varphi_k(x) = \exp\{-\frac{(\mathbf{x}_i - \boldsymbol{\mu}_k)^T(\mathbf{x}_i - \boldsymbol{\mu}_k)}{b_k^2}\}$. The activation functions are varying at each hidden unit due to the different centers $\boldsymbol{\mu}_k$. The $\gamma_{k,g}$'s are binary and control the inclusion of the neurons.

other subjects' treatment assignments.

3 Bayesian inference

We pursue a Bayesian approach to carry out the inference of the proposed RBF-net model with shared neurons, aiming to automatically quantify estimation uncertainty. In our model, $\{\Gamma, \boldsymbol{\mu}, \alpha, \boldsymbol{\theta}, \sigma, K\}$ is the complete set of parameters. Here, $\alpha \in \mathbb{R}$, $\sigma \in \mathbb{R}$, and $K \in \mathbb{R}$. As stated in Section 2, $\boldsymbol{\Gamma} = ((\gamma_{k,g}))_{1 \leq k \leq K, 1 \leq g \leq G}$ is a $K \times G$ dimensional binary matrix. The RBF-centers $\boldsymbol{\mu} = \{\boldsymbol{\mu}_1, \dots, \boldsymbol{\mu}_K\}$ is $P \times K$ dimensional matrix, where $\boldsymbol{\mu}_k = ((\mu_{p,k}))_{1 \leq p \leq P}$. α is the intercept, $\boldsymbol{\theta} = \{\theta_1, \dots, \theta_k\}$ is the K -length vector of coefficients, σ is the error standard deviation, and finally K is the total number of RBF-bases. Although K is unknown, we first specify the priors assuming a given value of K . In Section 3.4, our specification procedure for K is discussed following an empirical Bayes-type strategy.

3.1 Prior specification

To proceed with our Bayesian analysis, we put prior distributions on the parameters. We assume independent priors for $\mathbf{\Gamma}, \boldsymbol{\mu}, \alpha, \boldsymbol{\theta}, \sigma$. They are described below in detail.

1. The basis inclusion indicators ($\mathbf{\Gamma}$): The indicators are independent and follow Bernoulli distribution as $\gamma_{k,g} \sim \text{Bernoulli}(p_g)$ where $p_g \sim \text{Beta}(c, d)$.
2. The RBF-centers ($\boldsymbol{\mu}$): We put a multivariate normal distribution as the prior for $\boldsymbol{\mu}$, $\mu_{p,k} \sim \text{Normal}(0, \sigma_\mu^2)$.
3. The intercept and coefficients ($\alpha, \boldsymbol{\theta}$): We let both $\alpha, \theta_k \sim \text{Normal}(0, \sigma_d^2)$, with a pre-specified σ_d .
4. The error variance (σ): We specify a half-Cauchy prior for σ as $\sigma \sim C^+(0, \hat{\sigma})$.

The choice of the half-Cauchy distribution as prior for σ is motivated by Linero and Yang (2018). We set $\hat{\sigma}$ to be the error standard deviation from the linear regression model, where the outcome is regressed on the predictors and the treatment covariate as a factor. Further details on the hyperparameters c, d, σ_μ , and σ_d is provided in Section 3.5.

3.2 Likelihood function of data

In this section, we formalize the posterior likelihood function for our Bayesian inference model, considering both the observed data and the relevant parameters. The likelihood of our proposed model is

$$p(\mathbf{y}|\mathbf{\Gamma}, \boldsymbol{\mu}, \boldsymbol{\theta}, \alpha, \sigma) \propto \prod_i^N \prod_g^G \exp\left(-\frac{(y_i - f_g(\mathbf{x}_i))^2}{2\sigma^2}\right), \quad (4)$$

and with the prior specified in Section 3.1 of the main paper, we can formally write each prior as

$$p(\mathbf{\Gamma}) \propto \prod_g^G \prod_k^K p_g^{\gamma_{k,g}} (1 - p_g)^{1 - \gamma_{k,g}} \quad (5)$$

$$p(\boldsymbol{\mu}) \propto \prod_p^P \prod_k^K \exp\left(-\frac{\mu_{p,k}^2}{2\sigma_\mu^2}\right) \quad (6)$$

$$p(\boldsymbol{\theta}) \propto \prod_k^K \exp\left(-\frac{\theta_k^2}{2\sigma_d^2}\right) \quad (7)$$

$$p(\alpha) \propto \exp\left(-\frac{\alpha^2}{2\sigma_d^2}\right) \quad (8)$$

$$p(\sigma) \propto \left(\hat{\sigma} \left[1 + \left(\frac{\sigma}{\hat{\sigma}}\right)^2\right]\right)^{-1} \quad (9)$$

The full proportional posterior is then given by:

$$\begin{aligned} p(\boldsymbol{\Gamma}, \boldsymbol{\mu}, \boldsymbol{\theta}, \alpha, \sigma | \mathbf{y}) &\propto \prod_i^N \prod_g^G \prod_p^P \prod_k^K \left(\frac{1}{\sigma}\right) \exp\left(-\frac{(y_i - f_g(\mathbf{x}_i))^2 \sigma^2}{2\sigma^2}\right) \times p_g^{\gamma_{k,g}} (1 - p_g)^{1 - \gamma_{k,g}} \\ &\times \exp\left(-\frac{\mu_{p,k}^2}{2\sigma_\mu^2}\right) \times \exp\left(-\frac{\theta_k^2}{2\sigma_d^2}\right) \times \exp\left(-\frac{\alpha^2}{2\sigma_d^2}\right) \\ &\times \left(\hat{\sigma} \left[1 + \left(\frac{\sigma}{\hat{\sigma}}\right)^2\right]\right)^{-1} \end{aligned}$$

In the next subsections, we discuss our posterior sampling algorithms, the specification of the prior hyperparameters, and other related computational details.

3.3 Posterior sampling

We use superscript (t) to represent the corresponding posterior sample at the t -th iteration while describing the MH steps in detail below. Our sampler iterates between the following steps:

1. **Updating α , $\boldsymbol{\theta}$:** The parameter α is updated by sampling from a normal distribution, $\alpha \sim \text{Normal}(\alpha_0 \sigma_0, \sqrt{\sigma_0})$. Here, α_0 is defined as $\sum_i (y_i - f_g(\mathbf{x}_i)) / \sigma^2$, and σ_0 as $(\sigma_d^{-2} + N / \sigma^2)^{-1}$. The full conditional of $\boldsymbol{\theta}$ is $\text{Normal}(\tilde{\boldsymbol{\theta}}, \mathbf{D})$, where $\tilde{\boldsymbol{\theta}} = \mathbf{D} (\sigma_d^{-2} \boldsymbol{\theta}_0 + \mathbf{X}^{*T} \mathbf{R} / \sigma^2)$ and $\mathbf{D} = (\sigma_d^{-2} \mathbf{I}_K + \mathbf{X}^{*T} \mathbf{X}^* / \sigma^2)^{-1}$. Here we define $\boldsymbol{\theta}_0 = (0, \dots, 0)^T$ and \mathbf{X}^* as a $N \times K$ matrix, where the i, k -th entry is $X_{i,k}^* = \gamma_{k,g} \exp\{-(\mathbf{x}_i - \boldsymbol{\mu}_k)^T (\mathbf{x}_i - \boldsymbol{\mu}_k) / b_k^2\}$, in which g is the corresponding treatment group for the i -th patient. We let the vector $\mathbf{R} = (R_1, \dots, R_n)$ be the residuals $R_i = y_i - \alpha$.

In cases of large values of K , the above-mentioned sampling method for $\boldsymbol{\theta}$ may not be efficient, particularly when updating $\boldsymbol{\theta}$ from the full conditional where the k -th column of \mathbf{X}^* contains only 0. This condition implies that the corresponding k -th row of $\boldsymbol{\Gamma}$ is entirely 0. However,

there is a strategic approach to mitigate this potential issue. When the k -th row of $\mathbf{\Gamma} = 0$, the full conditional of $\boldsymbol{\theta}$ simplifies to the prior distribution. We can then use a two-part sampling strategy for $\boldsymbol{\theta}$. We create a set of indices \mathcal{Z} such that the z -th row in which $\mathbf{\Gamma}$ contains only 0 for all $z \in \mathcal{Z}$, and sample θ_z from the prior distribution $\text{Normal}(0, \sigma_d^2)$. Let \mathcal{Z}^c be the complement set of indices. We sample $\boldsymbol{\theta}_{\mathcal{Z}^c}$ from the conditional $\text{Normal}(\tilde{\boldsymbol{\theta}}_{\mathcal{Z}^c}, \mathbf{D}_{\mathcal{Z}^c})$. In this case $\tilde{\boldsymbol{\theta}}_{\mathcal{Z}^c} = \mathbf{D}_{\mathcal{Z}^c} (\sigma_d^{-2} \boldsymbol{\theta}_{0, \mathcal{Z}^c} + \mathbf{X}_{\mathcal{Z}^c}^{*T} \mathbf{R} / \sigma^2)$, where $\mathbf{X}_{\mathcal{Z}^c}^{*T}$ is the submatrix from \mathbf{X}^* with columns from \mathcal{Z}^c , and $\mathbf{D}_{\mathcal{Z}^c} = (\sigma_d^{-2} \mathbf{I}_{|\mathcal{Z}^c|} + \mathbf{X}_{\mathcal{Z}^c}^{*T} \mathbf{X}_{\mathcal{Z}^c}^* / \sigma^2)^{-1}$, where $|\mathcal{Z}^c|$ denotes the number of entries \mathcal{Z}^c . This approach reduces computation time for large values of K .

2. **Updating $\mathbf{\Gamma}$:** Here, we consider full conditional Gibbs updates, where we update $\gamma_{k,g}$ in random order. We update $\gamma_{k,g}$ by sampling from a Bernoulli distribution, $\gamma_{k,g} \sim \text{Bernoulli}(\tilde{p}_g)$, where $\tilde{p}_g = \frac{p_g l_g^1}{p_g l_g^1 + (1-p_g) l_g^0}$. Here l_g^1 is the model likelihood when $\gamma_{k,g} = 1$ and likewise, l_g^0 is the model likelihood when $\gamma_{k,g} = 0$.
3. **Updating p_g :** We sample $p_g \sim \text{Beta}(c + \sum_g \gamma_{k,g}, d + K - \sum_g \gamma_{k,g})$. However, as discussed in Section 3.4 of the main paper, some of the indices are kept fixed for the first 1000 iterations of the MCMC and thus, the above posterior distribution is marginally adjusted by excluding those fixed indices.

We now describe the updates for $(\sigma$ and $\boldsymbol{\mu}_k)$, employing the Metropolis-Hastings (MH) sampling algorithm. For σ , we use the MH step as proposed in Linero and Yang (2018), while for $\boldsymbol{\mu}_k$ a gradient-based Langevin Monte Carlo (LMC) sampling algorithm is adopted. This approach is beneficial for complex hierarchical Bayesian model. We use superscript (t) to represent the corresponding posterior sample at the t -th iteration while describing the MH steps in detail below.

1. **Updating σ :** We implement the updating technique from Linero and Yang (2018). When imposing a flat prior for σ^{-2} , we can show that the conditional distribution for σ^{-2} is $\sigma^{-2} \sim \text{Ga}(1+N/2, \sum_g \sum_{i \in g} (R_i - f_g(\mathbf{x}_i))^2)$, where Ga stands for the gamma distribution. Under a flat prior, we can let this full conditional be our proposal distribution. This idea enables there to be a simplification in the acceptance probability, in which the acceptance probability conveniently becomes the ratio of priors. However, in order to integrate the proposal distribution in the

standard MH algorithm, we need to adjust the acceptance probability with the Jacobian transformation. Thus, we can accept the proposal with probability

$$A\left(\sigma^{(t)} \rightarrow \sigma'\right) = \frac{C^+(\sigma' | 0, \hat{\sigma}) \sigma'^3}{C^+(\sigma^{(t)} | 0, \hat{\sigma}) \sigma^{(t)3}} \wedge 1 \quad (10)$$

2. **Updating μ_k :** To update μ_k , we use a gradient based sampler. The conditional posterior log-likelihood and its derivative with respect to $\mu_{p,k}$ are needed this process. The conditional posterior log-likelihood $\log P(\mu_k | \mathbf{y}, \mathbf{\Gamma}, \boldsymbol{\theta}, \alpha, \sigma)$ is

$$-\frac{n}{2} \log(2\pi\sigma^2) - \frac{1}{2\sigma^2} \sum_{i=1}^n (R_i - f_g(\mathbf{x}_i))^2 - \sum_{p=1}^P \frac{\mu_{p,k}^2}{2\sigma_\mu^2}.$$

The p -th entry of corresponding derivative $\nabla \log P(\mu_k | \mathbf{y}, \mathbf{\Gamma}, \boldsymbol{\theta}, \alpha, \sigma)$, with respect to $\mu_{p,k}$, is given by

$$\frac{2}{\sigma^2} \theta_k \gamma_{k,g} \sum_{i=1}^n \exp\left(-\sqrt{\frac{\sum_{p=1}^P (x_{i,p} - \mu_{p,k})^2}{b_k^2}}\right) \frac{\sum_{p=1}^P (x_{i,p} - \mu_{p,k})^2}{b_k^2} \left(\frac{x_{i,p} - \mu_{p,k}}{b_k^2}\right) - \frac{\mu_{p,k}}{\sigma_\mu^2}.$$

With gradient sampling, our proposed value now depends on the derivative, so that $\mu'_k = \mu_k^{(t)} + \frac{\epsilon}{2} \nabla \log P(\mu_k | \mathbf{y}, \mathbf{\Gamma}, \boldsymbol{\theta}, \alpha, \sigma) |_{\mu_k = \mu_k^{(t)}} + \delta$, where $\delta \sim \text{Normal}(0, \epsilon)$. Thus, the transition probability is

$$q(\mu'_k | \mu_k) \propto \exp\left(-\frac{1}{2\epsilon} \left\| \mu'_k - \mu_k - \frac{\epsilon}{2} \nabla \log P(\mu_k | \mathbf{y}, \mathbf{\Gamma}, \boldsymbol{\theta}, \alpha, \sigma) \right\|_2^2\right), \quad (11)$$

and then the acceptance probability for our gradient sampler for a proposed value μ' is

$$A\left(\mu_k^{(t)} \rightarrow \mu'_k\right) = \frac{P(\mu'_k | \mathbf{y}, \mathbf{\Gamma}, \boldsymbol{\theta}, \alpha, \sigma) q(\mu_k^{(t)} | \mu'_k)}{P(\mu_k^{(t)} | \mathbf{y}, \mathbf{\Gamma}, \boldsymbol{\theta}, \alpha, \sigma) q(\mu'_k | \mu_k^{(t)})} \wedge 1. \quad (12)$$

The proposal values for $\mu_{p,k}$ are adjusted to achieve a pre-specified acceptance rate, tuning ϵ every 200 iterations to maintain an acceptance rate between 0.45 and 0.7.

3.4 Specification of K

Our approach here relies on the empirical Bayes-type scheme, discussed in Roy (2023). We first create an index list to group the response and predictors associated with the g -th treatment. For each treatment group, we utilize Gaussian RBF kernel-based relevance vector machine (RVM) within the `rvm` function within the R package `kernlab` (Karatzoglou et al., 2004), which provides the group-specific number of relevance vectors v_g . We then set $K = G \times \max_g v_g$, combining all the outputs of `rvm`.

For initializing $\mathbf{\Gamma}$, we rely on both v_g and K . We first specify G disjoint sets, denoted as $\{\mathcal{I}_1, \dots, \mathcal{I}_G\}$. We have $\mathcal{I}_g \cap \mathcal{I}_{g'} = \emptyset$ for all $g \neq g'$ and $\cup_{g=1}^G \mathcal{I}_g \subset \{1, 2, \dots, K\}$. These are a small set of indices such that $\gamma_{k,g}$ is fixed at 1 for all $k \in \mathcal{I}_g$ at the initial stage of the MCMC. The set \mathcal{I}_g is constructed as $\mathcal{I}_g = \{k + \sum_{t=1}^{g-1} v_t : k \in \{1, 2, \dots, v_g\}\}$. For the first 1000 iterations, we only sample $\gamma_{k,g}$ for $k \notin \mathcal{I}_g$, and then for all k afterwards.

The initialization of the RBF centers $\boldsymbol{\mu}$ relies on the entropy-weighted k-means (EWKM) clustering algorithm, which incorporates an entropy-based weighting scheme on traditional k-means clustering. We implement the algorithm through the `ewkm` function from the `wskm` package in R (Williams et al., 2020), where we set K as the target number of centers. The function returns the centroids of the clusters, computed as the weighted mean position of all points in each cluster. To ensure stability, we add a small amount of random noise (from a normal distribution) to the centroids, as some initial centers are identical in the `ewkm` output. The final adjusted centroids serve as our initialization for $\boldsymbol{\mu}_k$'s and thus, $\boldsymbol{\mu}$.

3.5 Other computational settings

Our calibration of the prior hyperparameters follows some of the data-driven strategies proposed in Chipman et al. (2010) and Linero and Yang (2018). We first apply min-max transformation on the response as, $(\mathbf{y} - \min(\mathbf{y}) - 0.5(\max(\mathbf{y}) - \min(\mathbf{y}))) / (\max(\mathbf{y}) - \min(\mathbf{y}))$ which makes it bounded in $[-0.5, 0.5]$. After fitting the model, we apply an inverse transformation on the estimated f_g 's. The covariates \mathbf{x} , are similarly normalized to the range within $[0, 1]$ for continuous and ordinal variables. In the case of nominal categories with C levels, we form $C - 1$ binary dummy variables that do not need any further scaling. Here, we discuss our procedure for specifying the prior variance

σ_d^2 of θ_k when there are K_1 bases. Subsequently, we set a suitable value for K_1 based on $\gamma_{k,g}$'s. Under the RBF-net model, the expectation of a response given the covariate \mathbf{x} with K_1 bases is $\sum_{k=1}^{K_1} \theta_k \exp\{-(\mathbf{x} - \boldsymbol{\mu}_k)^T(\mathbf{x} - \boldsymbol{\mu}_k)/b_k^2\}$. For a random variable distributed as $\text{Normal}(\mu, \sigma^2)$, most of its mass falls within $\mu \pm 1.96\sigma$. Furthermore, the maximum value of $\exp\{-(\mathbf{x}_i - \boldsymbol{\mu}_k)^T(\mathbf{x}_i - \boldsymbol{\mu}_k)/b_k^2\}$ is 1. Thus, the value of $\sum_{k=1}^{K_1} \theta_k \exp\{-(\mathbf{x} - \boldsymbol{\mu}_k)^T(\mathbf{x} - \boldsymbol{\mu}_k)/b_k^2\}$ will be within $0 \pm 1.96\sigma_d\sqrt{K_1}$ if $\theta_k \sim \text{Normal}(0, \sigma_d^2)$. Our min-max normalized data satisfies $|y_{\min}| = |y_{\max}| = 0.5$. Thus, we may set $0.5 = 1.96\sigma_d\sqrt{K_1}$. Hence, approximately, $\sigma_d = 1/(4\sqrt{K_1}) = 1/(\sqrt{16K_1})$.

Now, in our case, the numbers of active bases are different for different $f_g(\cdot)$'s. For group g , we have $\sum_{k=1}^K \gamma_{k,g}$ bases. We, thus, consider to initialize K_1 as $K_1 = \max_g \sum_{k=1}^K \gamma_{k,g}$, based on our initialization of $\boldsymbol{\Gamma}$. One may also consider mean or median over g too, as we do not necessarily need K_1 to be an integer here. However, since this value may be inappropriate as parameters are updated, we recalculate K_1 during the burn-in phase of our MCM chain.

For parameter initialization, $\boldsymbol{\theta}$ is set as the least squares estimate. We initialize the probabilities $p_g = 1/2$ for all g , allowing an equal likelihood for all $k \in \mathcal{I}_g$, as described in Section 3.4, to be included. The bandwidth parameters b_k 's are also pre-specified. For simplicity, we let $b_k = b$ for all k . Then, we first initialize $\boldsymbol{\mu}$ as discussed in Section 3.4 and set: $b = \frac{\sqrt{2}}{k(k-1)} \sum_{i=1}^{k-1} \sum_{j=i+1}^k \|\boldsymbol{\mu}_i - \boldsymbol{\mu}_j\|_2$, where $\|\cdot\|_2$ represents the Euclidean norm and $\boldsymbol{\mu}_j$ is j -th column of $\boldsymbol{\mu}$. Some of the prior hyperparameters are set as $\sigma_\mu = 1, c = d = 1$.

3.6 Inference for CATE using linear projections and thresholding

Following Semenova and Chernozhukov (2021); Cui et al. (2023), we adopt a linear projection-based approach for the inference on $\tau(\cdot)$ to circumvent the difficulties in non-parametric inferences and provide a meaningful interpretation and summary of treatment heterogeneity, as argued in Semenova and Chernozhukov (2021). The best linear projection (BLP) of $\tau(\cdot)$ given a set of covariates \mathbf{x}_i is defined as

$$\{\beta_0^*, \boldsymbol{\beta}^*\} = \operatorname{argmin}_{\beta_0, \boldsymbol{\beta}} \mathbb{E} \left[(\tau(\mathbf{x}_i) - \beta_0 - \mathbf{x}_i \boldsymbol{\beta})^2 \right],$$

where β_0^* and $\boldsymbol{\beta}^*$ are the intercept and the coefficient estimates our covariates, respectively. One can estimate the BLP parameters by regressing the CATE estimates $\hat{\tau}(\mathbf{x}_i)$ on \mathbf{x}_i .

We modify this approach for our Bayesian setting with three treatments in our numerical

experiment and MIMIC data application. For example, we may consider τ_{21} and τ_{31} , comparing treatments 2 and 3 with treatment 1, respectively. Then, for the b -th posterior sample, we obtain $\tau_{21,b}(\mathbf{x}_i)$ and $\tau_{31,b}(\mathbf{x}_i)$, based on the posterior samples of f_g 's for the i -th patient. We next separately regress $\tau_{21,b}(\mathbf{x})$ and $\tau_{31,b}(\mathbf{x})$ on \mathbf{x} , providing the estimated BLP coefficients for each predictor.

Furthermore, we propose thresholding the BLP coefficients and computing the credible intervals. We generate B posterior samples and then compute the BLP coefficient $\beta_p^{(b)}$ for each predictor p and posterior sample b . Finally, for a given predictor p and threshold t , we compute $s_{p,t} = \frac{1}{B} \sum_{b=1}^B \mathbf{1}\{|\beta_p^{(b)}| > t\}$, the proportion of coefficients falling outside of the interval $(-t, t)$ across all the posterior samples. A larger value of $s_{p,t}$ would indicate the higher importance of p -th predictor under a given level of threshold t . It is easy to see that as t increases, $s_{p,t}$ will decrease. A slower decay in $s_{p,t}$ with increasing t indicates greater importance, providing us a measure for comparing importances of different predictors.

It is important to note that the BLPs are not posterior samples of any model parameter. They are estimated based on a loss minimization and can be expressed as a fixed function of the posterior samples. Specifically, the function here is a linear function $h(\mathbf{z}) = \mathbf{A}\mathbf{z}$, where $\mathbf{A} = \mathbf{X}(\mathbf{X}^T\mathbf{X})^{-1}\mathbf{X}^T$ and \mathbf{X} is the $n \times p$ design matrix with n observations and p predictors. For b -th posterior sample and (g, g') pair of treatments, we set $\mathbf{z} = \{\tau_{gg',b}(\mathbf{x}_i)\}_{i=1}^n$ and compute $h(\mathbf{z})$ to get the BLPs. The proposed BLP-based approach works surprisingly well in Section 4.2. However, it should be used with caution.

4 Simulation

In this section, we assess the effectiveness of our proposed RBF method by estimating model parameters using the training data and calculating predicted mean square errors on the test set. The mean square error (MSE) for treatment-groups pair (g, g') is defined as $\frac{1}{|T_r|} \sum_{i \in T_r} (\tau_{gg'}(\mathbf{x}_i) - \hat{\tau}_{gg'}(\mathbf{x}_i))^2$, where T_r represents the test set for the r -th replication. We then compute the median MSE over r for each method. Here, $\hat{\tau}_{gg'}(\mathbf{x}_i)$ represents the posterior mean for the Bayesian implementations and the point estimate for the frequentist implementations of $\tau_{gg'}(\mathbf{x}_i)$, respectively. We conduct two simulations with 50 replications.

In each case, we compare our estimates with a multi-arm causal forest from the `grf` (Tib-

shirani et al., 2023) package-based solution. For CATE estimation (Tibshirani et al., 2023), `multi_arm_causal_forest` and `predict.multi_arm_causal_forest` functions are applied on the training and testing set, respectively. To the best of our knowledge, there is no other package that supports CATE estimation for more than two treatments for out-of-sample predictors. Additionally, we compare these results with other methods using T-learning and S-learning. We employ T-learning by fitting treatment-specific functions. For S-learning with three treatments, we model the outcome $y_i = f(\mathbf{x}_i, z_{2i}, z_{3i}) + \epsilon_i$, where $z_{2i} = 1$ if i -th subject is treated under the second treatment and zero otherwise; z_{3i} is defined similarly for the third treatment. Consequently, z_{2i} and z_{3i} are both zero if i -th subject is in the first treatment group.

Our candidate models for both approaches are relevance vector machine (RVM), support vector regression (SVR), ordinary least square (OLS), and BART, using the corresponding R packages `e1071R` (Meyer et al., 2019), `kernlab` (Karatzoglou et al., 2004), `BART`(McCulloch et al., 2019), and few other functions from the base packages of R.

The outcome \mathbf{y} is generated by y_i from $\text{Normal}(f_g(\mathbf{x}_i), 1)$, where three treatment-outcome functions $f_1(\cdot), f_2(\cdot), f_3(\cdot)$ are

$$\begin{aligned} f_1(\mathbf{x}) &= f_1^0(\mathbf{x}) + f_2^0(\mathbf{x}), \\ f_2(\mathbf{x}) &= (f_1^0(\mathbf{x}) + f_2^0(\mathbf{x}))/2 + f_3^0(\mathbf{x})/3, \\ f_3(\mathbf{x}) &= (f_2^0(\mathbf{x}) + f_3^0(\mathbf{x}))/2 + f_1^0(\mathbf{x})/3, \end{aligned}$$

where

$$\begin{aligned} f_1^0(\mathbf{x}) &= 10 \sin(\pi x_1 x_2) + 20(x_3 - 0.5)^2 + (10x_4 + 5x_5), \\ f_2^0(\mathbf{x}) &= (5x_2)/(1 + x_1^2) + 5 \sin(x_3 x_4) + x_5, \\ f_3^0(\mathbf{x}) &= 0.1 \exp(4x_1) + 4/(1 + \exp(-20(x_2 - 0.5))) + 3x_3^2 + 2x_4 + x_5. \end{aligned}$$

4.1 Setting 1

Under this setting, we consider two sample sizes 180 and 360 with three equal treatment groups. To assess the performance of our model, each dataset is partitioned into training and testing sets with a 67/33 split.

The results, as detailed in Table 1, demonstrate the efficacy of our proposed method. Notably, our approach consistently outperforms both S-learning and T-learning-type models, where treatment-specific separate outcome functions are fitted. This is particularly evident in the scenario with the smaller sample size. Compared to the multi-arm causal forest, our method demonstrates superior performance in the smaller sample size case, while results are comparable for larger sample sizes. This indicates that our model is particularly effective with limited data, an important advantage for practical applications where large datasets may be scarce.

4.2 Setting 2

In Setting 1, the assignment of the treatment groups and the generation of the predictors are performed independently. We now use the MIMIC-III database to evaluate our model with unknown, real-world complexities in predictor-treatment dependencies. From the dataset, we constructed three treatment groups based on the usage of only mechanical ventilation (group 1), only vasopressor (group 2), and both (group 3), as detailed in Section 5. Our final dataset in our real data analysis comprises of 172 subjects and 15 predictors but for this simulation, we use a subset of predictors. Employing the marginal screening approach from Xue and Liang (2017), we pick the top five most important predictors for each of the two outcomes: the length of stay in the Intensive Care Unit (LOS-ICU) and Sequential Organ Failure Assessment (SOFA) scores. After taking the union, we find the following set of seven key predictors: age, weight, bicarbonate level, sodium level, systolic blood pressure (SBP), potassium level, and mean arterial pressure (MAP).

We then generate \mathbf{y} in the same manner as in the preceding section based on the first five predictors(excluding potassium and MAP), but fit the model with all seven to evaluate their importance subsequently. We want to mention here that the marginal screening procedure is not essential for this simulation but is used systematically to ensure we include the most important predictors associated with the primary outcomes in Section 5. This approach enables complex associations

between predictors and treatment assignments, as they are also borrowed from MIMIC data.

Table 2 presents an MSE comparison of the CATE estimates of our method versus other competing methods. As in the smaller sample size case of Section 4.1, our model consistently outperforms the multi-arm causal forest, and among S and T-learning methods, our method excels except for the marginally better performance by support vector regression under T-learning.

Since the outcome \mathbf{y} depends on only the first five predictors, we turn to our thresholding-based credible interval comparison approach from Section 3.6 to analyze the $s_{p,t}$ -values for different predictors (p) and threshold (t), ranging from 0.1 to 2.0. Table 3 shows the $s_{t,p}$ -values based on 50 replications for τ_{23} and τ_{13} , respectively. As expected, the decrease in $s_{p,t}$ with t is the sharpest for potassium and MAP, which aligns with their exclusion from the data generation process. The $s_{p,t}$ -values thus provide useful insights into the relationship between the outcome and the predictors.

Here, we show that even flexible methods effective in treatment-effect estimation may underperform if the response curves share common characteristics. For example, while the RVM model with a Gaussian kernel resembles our RBF model, both T and S learning implementations of RVM are less efficient than the shared-kernel model. Since treatments often share commonalities, our proposed method with shared bases outperforms alternatives lacking shared structural features.

5 MIMIC Data Analysis

MIMIC-III is a large single-center database, containing deidentified, comprehensive clinical data of 53,423 adult ICU patient admissions from 2001 to 2012 at Beth Israel Deaconess Medical Center in Boston, Massachusetts (Johnson et al., 2016). The dataset offers a vast amount of patient information, encompassing demographics, laboratory results, medicine summaries, and diagnostic codes. This extensive data allows us to employ our RBF-net with shared neurons for septic patients. With the most current revision, sepsis is defined following Singer et al. (2016) as a life-threatening condition resulting from dysregulated host responses to infection, often identified by a Sequential [Sepsis-related] Organ Failure Assessment (SOFA) score increase of 2 points or more. Its progression can lead to septic shock, marked by severe circulatory and metabolic dysfunction. Our analysis focuses on septic patients’ data from the first 12 hours of their initial visit, excluding readmissions. We define sepsis based on diagnoses of “Sepsis”, “Septic shock”, or “Severe sepsis” during their

inaugural visit and include only those discharged to their “home.”

One challenge regarding MIMIC-III, and electronic health records in general, is the amount of missing data (Groenwold, 2020). To handle missing data in MIMIC-III (Hou et al., 2020), we exclude variables with more than 20% missing data and apply a hybrid procedure: first, the last observation carried forward (LOCF) using the `na.locf` function from the R package `zoo` (Zeileis and Grothendieck, 2005), followed by multiple imputations for patients who do not have observations in the initial hours of their visit. We consider multiple imputations using the R package `mice` (van Buuren and Groothuis-Oudshoorn, 2011).

The set of predictors considered in our analysis are age, weight, hemoglobin, white blood cells, blood urea nitrogen (BUN), potassium, sodium, bicarbonate, creatinine, platelet count, heart rate, systolic blood pressure (SBP), diastolic blood pressure (DBP), mean arterial pressure (MAP), and temperature. As discussed in Section 4.2, our treatment groups are based on the usage of only mechanical ventilation (group 1), only vasopressor (group 2), and both (group 3). Tables 4 and 5 are the demographics for our study population, with Table 5 stratifying by treatment group. The demographics contain the mean and standard deviation of both the predictors and outcomes.

For our analysis, we consider two possible outcomes, the length of ICU stay and the 12-*th* hour SOFA score. We initially fit the model for both of the two outcomes in their original scale and the log scale. However, after examining the distributions of the residuals, we only consider reporting our results for the LOS-ICU in log scale and SOFA scores with a square root transformation as their residuals uphold the normality assumption. To further confirm this, we perform the Shapiro-Wilks test using `shapiro.test` in R. The residual density plots are provided in Figures 1 and 2 in the supplementary material.

For each choice of outcome, we obtain $s_{p,t}$ -values along with the BLPs for each covariate along for both $\hat{\tau}_{23}$ and $\hat{\tau}_{13}$. The $s_{p,t}$ values illustrated in Section 3.6 are presented in Table 6 for different predictors (p) and thresholds (t) up to 0.3. For LOS-ICU, heart rate, MAP, and SBP show the highest $s_{p,t}$ -values for $\hat{\tau}_{23}$, whereas most predictors for $\hat{\tau}_{13}$ experience a significant drop-off, leaving heart rate as the only predictor with non-zero $s_{p,t}$ -values at higher thresholds. When analyzing SOFA score, predictors such as bicarbonate, creatinine, MAP, platelet count, and SBP exhibit the largest $s_{p,t}$ -values in both $\hat{\tau}_{23}$ and $\hat{\tau}_{13}$. Notably, platelet count has non-zero $s_{p,t}$ -values at threshold 0.3 for both $\hat{\tau}_{23}$ and $\hat{\tau}_{13}$. The BLP coefficients for these important predictors are presented in Table

7. For LOS-ICU, heart rate and MAP both have negative BLP coefficients. In contrast, SBP has a positive BLP coefficient. For the square-root transformed SOFA score, the BLP coefficients of platelet count and SBP are both positive. whereas, MAP has a negative coefficient. Their implications are further discussed in the context of optimal treatments in Section 6.

6 Discussion

Our findings indicate that the four physiological predictors MAP, SBP, heart rate, and platelet count may be the most important predictors for the two outcomes of interest. For both outcomes, a positive BLP coefficient indicates that administering both vasopressors and mechanical ventilation is preferred, while a negative coefficient suggests that either vasopressor or mechanical ventilation alone is preferable, depending on the specific context. For instance in LOS-ICU, heart rate and MAP both have negative BLP coefficients for $\hat{\tau}_{23}$, indicating that patients with higher heart rate or MAP should receive vasopressors alone, as it is associated with shorter ICU stays. On the other hand, the positive coefficient of SBP suggests that a combination of vasopressor and mechanical ventilation is more beneficial for patients with higher SBP. For SOFA scores, platelet count and SBP both have positive BLP coefficients for $\hat{\tau}_{23}$, suggesting that patients with higher values of these predictors would benefit from receiving both treatments, as this combination may lead to better outcomes in terms of SOFA scores. Conversely, the negative BLP coefficient for MAP in the SOFA score context indicates that patients with higher MAP should receive mechanical ventilation alone to reduce their SOFA scores. These findings align with previous studies that show how these predictors affect LOS-ICU and SOFA scores (Li et al., 2024; Khanna et al., 2023; He et al., 2022; Zhang et al., 2022).

For our inference, we proposed a Bayesian version of the BLP approach (Semenova and Chernozhukov, 2021) with thresholding. However, it may be too simple to reflect the heterogeneity in the CATE. Recently, Shin et al. (2024) proposed a kernel-based approach for a similar problem but with an increased computational demand. Nevertheless, it will be useful to consider this approach in the future.

Looking ahead, we hope to potentially broaden our model’s application. The shared basis construction can be generalized to other types of models as well. Like in tree-based models, one

may allow sharing of trees. Another direction will be to extend the proposed architecture to model other types of outcomes, such as right-censored survival data or binary or count-valued data. Another possible extension of the proposed model is to incorporate the covariate effect into p_g . They may help to further the scope and impact of our work, particularly in the field of personalized medicine.

Acknowledgement

We thank the Editor, Associate Editor, and referee for the insightful comments that led to improvements in the content and presentation of the paper.

Supplementary materials

Supplementary materials some additional figures referenced in the main paper.

Conflict of interest

None declared.

Data availability

The Medical Information Mart for Intensive Care III (MIMIC-III) data are available through Physionet (mimic.physionet.org). The codes to run the model are available at <https://github.com/pshuwei/RBF> along with specific implementation codes for each simulation.

Table 1: Comparing estimation errors for the two treatment contrasts τ_{21} and τ_{31} across different methods, based on 50 replications and two choices for the total sample size under Simulation setting 1. The errors for the S-learning and T-learning type models are separated from the two multi-treatment cases with a horizontal line. The reported errors are the medians over all replications, with the corresponding ranges in parentheses.

	$n = 180$		$n = 360$	
	$\hat{\tau}_{21}$ MSE	$\hat{\tau}_{31}$ MSE	$\hat{\tau}_{21}$ MSE	$\hat{\tau}_{31}$ MSE
Shared-neuron RBF	2.99 (2.36, 4.49)	4.84 (4.19, 5.94)	3.45 (2.89, 4.85)	4.51 (3.99, 5.41)
Causal Random Forest	5.32 (5.01, 6.34)	9.9 (9.34, 10.61)	2.54 (2.18, 2.88)	5.41 (4.73, 6.27)
RVM (S)	5.34 (3.28, 35.01)	10.3 (5.88, 13.37)	6.95 (3.2, 10.81)	7.22 (4.77, 10.49)
SVR (S)	5.11 (3.51, 10.13)	7.34 (4.93, 10.41)	6.29 (4.5, 7.59)	7.75 (6.61, 10.76)
OLS (S)	7.3 (6.36, 8.76)	10.25 (10.13, 10.66)	10.24 (9, 11.57)	11.54 (10.74, 12.46)
BART20 (S)	4.43 (2.82, 8.88)	9.11 (6.13, 12.74)	8.66 (5.58, 11.91)	8.86 (4.82, 12.16)
BART50 (S)	3.26 (2.21, 4.5)	8.07 (7.27, 9.33)	5.02 (3.66, 7.84)	5.56 (3.85, 7.77)
BART200 (S)	3.63 (3.03, 4.15)	8.61 (8.22, 9.11)	2.07 (1.54, 2.58)	4.69 (3.94, 5.39)
RVM (T)	14.03 (11.05, 19.75)	10.96 (9.3, 13.62)	8.71 (7.81, 12.1)	9.75 (7.04, 12.78)
SVR (T)	5.68 (3.91, 9.82)	7.11 (5.23, 9.48)	8.87 (7.01, 11.22)	8.98 (6.79, 11.92)
OLS (T)	8.8 (6.16, 12.45)	9.01 (6.48, 12.27)	4.97 (3.98, 6.61)	5.93 (4.74, 8.19)
BART20 (T)	14.55 (11.28, 17.96)	8.8 (6.3, 12.24)	11.14 (8.8, 14.27)	9.47 (6.25, 11.67)
BART50 (T)	14.59 (11.63, 17.92)	8.19 (5.86, 11.03)	10.16 (8.41, 12.59)	8.38 (5.93, 10.19)
BART200 (T)	15.07 (11.66, 18.24)	8 (6.1, 10.99)	10.85 (9.06, 13.19)	8.48 (6.33, 10.09)

Table 2: Comparing estimation errors for the two treatment contrasts τ_{23} and τ_{13} across different methods, based on 50 replications and two choices for the total sample size under Simulation setting 2. The errors for the S-learning and T-learning type models are separated from the two multi-treatment cases with a horizontal line. The reported errors are the medians over all replications, with the corresponding ranges in parentheses.

	$\hat{\tau}_{23}$ MSE	$\hat{\tau}_{13}$ MSE
Shared-neuron RBF	2.97 (2.37, 4.07)	4.28 (2.47, 6.73)
Causal Random Forest	4.67 (4.6, 5.35)	10.28 (6.93, 14.03)
RVM (S)	4.53 (3.65, 53.73)	10.35 (6.48, 47.12)
SVR (S)	11.21 (10.37, 13.21)	13.89 (10.75, 18.9)
OLS (S)	4.82 (4.79, 5.22)	8.06 (5.57, 10.6)
BART20 (S)	2.97 (2.3, 3.61)	9.1 (5.2, 13.24)
BART50 (S).	3.29 (2.56, 4.03)	11.67 (7.35, 16.69)
BART200 (S)	3.85 (3.31, 5.02)	13.08 (8.49, 17.6)
RVM (T)	12.99 (8.52, 20.08)	9.91 (7.25, 14.64)
SVR (T)	2.63 (1.7, 4.62)	3.87 (2.3, 6.36)
OLS (T)	6.51 (4.43, 9.76)	9.57 (6.09, 13.39)
BART20 (T)	11.1 (5.94, 17.15)	12.47 (9, 19.57)
BART50 (T)	10.46 (6.51, 16.73)	12.15 (8.77, 15.57)
BART200 (T)	9.7 (6.75, 15.38)	11.72 (8.56, 15.45)

Table 3: Comparison of thresholding-based $s_{p,t}$ -values for $\hat{\tau}_{23}$ and $\hat{\tau}_{13}$ for different choices of thresholds (t), and predictors. The thresholding levels are given in the first column. The generated outcomes are independent of the last two predictors. The exclusion proportions are based on 50 replicated datasets.

$\hat{\tau}_{23}$	Intercept	SBP	Bicarbonate	Sodium	Age	Weight	Potassium	MAP
0.1	1.00	1.00	1.00	1.00	1.00	1.00	0.95	1.00
0.2	1.00	1.00	1.00	1.00	1.00	1.00	0.89	1.00
0.3	1.00	1.00	1.00	1.00	1.00	1.00	0.84	1.00
0.4	1.00	1.00	1.00	0.99	1.00	1.00	0.79	1.00
0.5	1.00	1.00	1.00	0.99	1.00	1.00	0.74	0.99
0.6	1.00	0.99	1.00	0.99	1.00	1.00	0.69	0.99
0.7	1.00	0.99	1.00	0.99	1.00	1.00	0.64	0.99
0.8	1.00	0.99	1.00	0.99	1.00	1.00	0.59	0.98
0.9	1.00	0.99	1.00	0.98	1.00	1.00	0.55	0.97
1.0	1.00	0.99	1.00	0.98	1.00	1.00	0.50	0.96
1.1	1.00	0.99	1.00	0.97	1.00	1.00	0.46	0.95
1.2	1.00	0.98	1.00	0.97	1.00	1.00	0.42	0.93
1.3	1.00	0.98	1.00	0.96	1.00	0.99	0.38	0.91
1.4	1.00	0.98	1.00	0.96	1.00	0.99	0.34	0.88
1.5	1.00	0.98	1.00	0.95	1.00	0.99	0.30	0.84
1.6	1.00	0.97	1.00	0.94	1.00	0.99	0.27	0.80
1.7	1.00	0.97	1.00	0.93	1.00	0.99	0.24	0.76
1.8	1.00	0.97	1.00	0.92	1.00	0.99	0.21	0.70
1.9	0.99	0.96	1.00	0.91	1.00	0.98	0.19	0.65
2.0	0.99	0.96	1.00	0.89	1.00	0.98	0.16	0.59
$\hat{\tau}_{13}$								
0.1	1.00	1.00	1.00	1.00	1.00	1.00	0.95	1.00
0.2	1.00	1.00	1.00	1.00	1.00	1.00	0.90	1.00
0.3	1.00	1.00	1.00	1.00	1.00	1.00	0.84	1.00
0.4	1.00	1.00	1.00	1.00	1.00	1.00	0.79	0.99
0.5	1.00	1.00	1.00	0.99	1.00	1.00	0.74	0.99
0.6	1.00	1.00	1.00	0.99	1.00	1.00	0.69	0.98
0.7	1.00	1.00	1.00	0.99	1.00	1.00	0.64	0.98
0.8	1.00	0.99	1.00	0.99	1.00	1.00	0.59	0.97
0.9	1.00	0.99	1.00	0.98	1.00	1.00	0.54	0.96
1.0	1.00	0.99	1.00	0.98	1.00	1.00	0.49	0.94
1.1	1.00	0.99	1.00	0.98	1.00	1.00	0.45	0.93
1.2	1.00	0.99	1.00	0.97	1.00	1.00	0.41	0.90
1.3	1.00	0.99	1.00	0.97	1.00	1.00	0.37	0.87
1.4	1.00	0.99	1.00	0.96	1.00	1.00	0.33	0.84
1.5	1.00	0.99	1.00	0.95	1.00	0.99	0.29	0.79
1.6	1.00	0.98	1.00	0.94	1.00	0.99	0.26	0.75
1.7	1.00	0.98	1.00	0.93	1.00	0.99	0.23	0.69
1.8	1.00	0.98	1.00	0.92	1.00	0.99	0.20	0.64
1.9	1.00	0.98	1.00	0.91	1.00	0.99	0.17	0.58
2.0	1.00	0.97	1.00	0.89	1.00	0.98	0.15	0.52

Table 4: Overall Demographics for Selected Septic Patients in MIMIC-III Database. Predictor variables reported represent the average value after 12 hours of observation in hospital. Outcome variables reported represent the value at the 12th hour. We also report the amount of missing values in each group before applying LOCF and imputation to complete the data.

Overall		
Variable	Mean (SD)	% Missing
Age	53.8 (17.78)	0%
Bicarbonate	20.04 (4.15)	4.65%
BUN	25.43 (18.68)	4.65%
Creatinine	1.58 (1.54)	4.65%
DBP	60.57 (8.67)	0%
Hemoglobin	10.86 (1.81)	7.56%
Heart Rate	93.26 (17.91)	0%
Potassium	4.04 (0.67)	4.65%
Platelet Count	191.86 (104.14)	7.56%
MAP	73.74 (9.15)	0%
SBP	107.58 (11.97)	0%
Sodium	138.86 (3.6)	5.23%
Temperature	37.06 (0.82)	0%
Weight	82.29 (21.67)	2.91%
White Blood Cell	14.9 (8.44)	8.14%
Length of Stay in ICU	4.47 (4.01)	0%
SOFA Score	6.96 (2.82)	0%

Table 5: Treatment group-specific summaries of the covariates for selected sets of septic patients in the MIMIC-III database are illustrated here. For all the predictor variables, the reported statistics are based on the first 12-hour averages under ICU. The statistics on the SOFA score are evaluated based on the value at the 12th hour in the ICU.

	Ventilator Only	Vasopressor Only	Both
Variable	Mean (SD)	Mean (SD)	Mean (SD)
Age	53.88 (19.41)	46.7 (16.18)	57.49 (16.63)
Bicarbonate	18.96 (4.79)	21.48 (4.91)	19.85 (3.02)
BUN	28.96 (21.08)	23.84 (22.50)	24.13 (14.44)
Creatinine	1.68 (1.06)	1.42 (1.56)	1.62 (1.76)
DBP	59.78 (8.87)	64.56 (9.72)	59.01 (7.48)
Hemoglobin	11.4 (2.28)	10.82 (1.73)	10.58 (1.50)
Heart Rate	93.96 (18.48)	99.72 (18.78)	89.57 (16.27)
Potassium	4.23 (0.78)	4.07 (0.62)	3.88 (0.60)
MAP	73.27 (9.07)	79.62 (11.58)	71.07 (5.84)
Sodium	138.71 (4.02)	139.21 (4.34)	138.84 (3)
Platelet Count	191.44 (89.81)	212.27 (128.32)	181.59 (98.06)
SBP	105.43 (8.76)	117.01 (16.85)	104.17 (6.96)
Temperature	37.02 (0.82)	37.19 (0.76)	37.0 (0.76)
White Blood Cell	13.36 (7.41)	15.06 (9.12)	15.65 (8.72)
Weight	84.99 (26.85)	86.15 (25.24)	78.95 (15.51)
Length of Stay in ICU	6.14 (3.91)	6.43 (5.5)	2.48 (1.39)
SOFA Score	8.98 (2.82)	6.05 (2.8)	6.28 (2.22)

Table 6: Comparison of exclusion proportions for thresholding-based $s_{p,t}$ -values for $\hat{\tau}_{23}$ and $\hat{\tau}_{13}$ for $\log(\text{LOS-ICU})$ and $\sqrt{\text{SOFA Score}}$ for different choices of thresholds (t), and predictors. The thresholding levels are given in the first row. Treatment groups are based on the usage of only mechanical ventilation (group 1), only vasopressor (group 2), and both (group 3).

$\log(\text{LOS-ICU})$												
Variable	$\hat{\tau}_{23}$						$\hat{\tau}_{13}$					
	0	0.1	0.15	0.2	0.25	0.3	0	0.1	0.15	0.2	0.25	0.3
Intercept	1.00	0.94	0.92	0.89	0.85	0.82	0.99	0.46	0.34	0.23	0.16	0.12
Age	1.00	0.59	0.41	0.23	0.11	0.04	0.99	0.04	0.00	0.00	0.00	0.00
Bicarbonate	1.00	0.43	0.21	0.08	0.02	0.00	0.99	0.01	0.00	0.00	0.00	0.00
BUN	1.00	0.44	0.20	0.05	0.01	0.00	0.99	0.00	0.00	0.00	0.00	0.00
Creatinine	1.00	0.48	0.33	0.22	0.14	0.08	0.99	0.01	0.00	0.00	0.00	0.00
DBP	1.00	0.57	0.41	0.24	0.12	0.03	0.99	0.04	0.00	0.00	0.00	0.00
Hemoglobin	1.00	0.57	0.39	0.18	0.07	0.02	0.99	0.06	0.01	0.00	0.00	0.00
Heart Rate	1.00	0.79	0.68	0.56	0.46	0.36	0.99	0.24	0.12	0.05	0.02	0.01
MAP	1.00	0.87	0.76	0.60	0.45	0.27	0.99	0.03	0.00	0.00	0.00	0.00
Potassium	1.00	0.50	0.23	0.07	0.02	0.00	0.99	0.00	0.00	0.00	0.00	0.00
Platelet Count	1.00	0.57	0.39	0.21	0.09	0.02	0.99	0.00	0.00	0.00	0.00	0.00
SBP	1.00	0.81	0.72	0.60	0.49	0.35	0.99	0.04	0.01	0.00	0.00	0.00
Sodium	1.00	0.49	0.30	0.14	0.05	0.01	0.99	0.01	0.00	0.00	0.00	0.00
Temperature	1.00	0.43	0.20	0.06	0.01	0.00	0.99	0.00	0.00	0.00	0.00	0.00
Weight	1.00	0.52	0.30	0.13	0.03	0.00	0.99	0.00	0.00	0.00	0.00	0.00
White Blood Cell	1.00	0.54	0.41	0.25	0.12	0.05	0.99	0.00	0.00	0.00	0.00	0.00
$\sqrt{\text{SOFA Score}}$												
Intercept	1.00	0.79	0.71	0.64	0.55	0.46	1.00	0.82	0.74	0.67	0.60	0.52
Age	1.00	0.03	0.00	0.00	0.00	0.00	1.00	0.05	0.00	0.00	0.00	0.00
Bicarbonate	1.00	0.36	0.15	0.05	0.02	0.00	1.00	0.32	0.12	0.04	0.01	0.00
BUN	1.00	0.13	0.02	0.00	0.00	0.00	1.00	0.30	0.12	0.05	0.01	0.00
Creatinine	1.00	0.29	0.12	0.05	0.01	0.00	1.00	0.51	0.35	0.22	0.12	0.07
DBP	1.00	0.01	0.00	0.00	0.00	0.00	1.00	0.03	0.00	0.00	0.00	0.00
Hemoglobin	1.00	0.03	0.00	0.00	0.00	0.00	1.00	0.04	0.00	0.00	0.00	0.00
Heart Rate	1.00	0.02	0.00	0.00	0.00	0.00	1.00	0.06	0.00	0.00	0.00	0.00
MAP	1.00	0.22	0.01	0.00	0.00	0.00	1.00	0.47	0.09	0.00	0.00	0.00
Potassium	1.00	0.08	0.01	0.00	0.00	0.00	1.00	0.20	0.06	0.01	0.00	0.00
Platelet Count	1.00	0.43	0.24	0.11	0.05	0.02	1.00	0.56	0.38	0.26	0.15	0.08
SBP	1.00	0.63	0.17	0.01	0.00	0.00	1.00	0.75	0.33	0.05	0.00	0.00
Sodium	1.00	0.00	0.00	0.00	0.00	0.00	1.00	0.00	0.00	0.00	0.00	0.00
Temperature	1.00	0.01	0.00	0.00	0.00	0.00	1.00	0.01	0.00	0.00	0.00	0.00
Weight	1.00	0.04	0.00	0.00	0.00	0.00	1.00	0.03	0.00	0.00	0.00	0.00
White Blood Cell	1.00	0.02	0.00	0.00	0.00	0.00	1.00	0.02	0.00	0.00	0.00	0.00

Table 7: The BLP coefficients for predictors in MIMIC-III for $\tau_{23}(\mathbf{x})$ and $\tau_{13}(\mathbf{x})$ for log-transformed length of stay in the ICU and square-root transformed 12-th hour SOFA score. Treatment groups are based on the usage of only mechanical ventilation (group 1), only vasopressor (group 2), and both (group 3).

Variable	$\hat{\tau}_{23}$		$\hat{\tau}_{13}$	
	log(LOS-ICU)	$\sqrt{\text{SOFA Score}}$	log(LOS-ICU)	$\sqrt{\text{SOFA Score}}$
Intercept	-0.77	-0.52	-0.04	-0.17
Age	0.08	0.02	0.00	-0.02
Bicarbonate	-0.01	-0.04	0.00	-0.01
BUN	-0.00	0.00	-0.00	-0.02
Creatinine	-0.09	-0.05	-0.01	-0.05
DBP	-0.07	-0.03	0.00	-0.00
Hemoglobin	0.07	0.01	0.00	-0.02
Heart Rate	-0.23	-0.13	-0.01	-0.03
MAP	-0.23	-0.15	-0.01	-0.05
Potassium	0.03	0.02	0.00	-0.01
Platelet Count	0.09	0.03	0.00	0.03
SBP	0.22	0.17	0.01	0.07
Sodium	-0.07	-0.03	0.00	0.00
Temperature	0.01	-0.01	-0.00	-0.00
Weight	0.03	0.03	0.00	0.01
White Blood Cell	0.11	0.04	0.00	-0.01

References

- Brown, D. W., DeSantis, S. M., Greene, T. J., Maroufy, V., Yaseen, A., Wu, H. et al. (2020), “A novel approach for propensity score matching and stratification for multiple treatments: Application to an electronic health record–derived study,” *Statistics in medicine*, 39(17), 2308–2323.
- Chalkou, K., Steyerberg, E., Egger, M., Manca, A., Pellegrini, F., and Salanti, G. (2021), “A two-stage prediction model for heterogeneous effects of treatments,” *Statistics in medicine*, 40(20), 4362–4375.
- Cheng, D., Chakraborty, A., Ananthakrishnan, A. N., and Cai, T. (2020), “Estimating average treatment effects with a double-index propensity score,” *Biometrics*, 76(3), 767–777.
- Chernozhukov, V., Chetverikov, D., Demirer, M., Duflo, E., Hansen, C., Newey, W., and Robins, J. (2018), “Double/debiased machine learning for treatment and structural parameters,” *The Econometrics Journal*, 21(1), C1–C68.
- Chipman, H. A., George, E. I., and McCulloch, R. E. (2010), “BART: Bayesian additive regression trees,” *The Annals of Applied Statistics*, 4(1), 266–298.
- Cui, Y., Kosorok, M. R., Sverdrup, E., Wager, S., and Zhu, R. (2023), “Estimating heterogeneous treatment effects with right-censored data via causal survival forests,” *Journal of the Royal Statistical Society Series B: Statistical Methodology*, 85(2), 179–211.
- Cui, Y., and Tchetgen Tchetgen, E. (2021), “A semiparametric instrumental variable approach to optimal treatment regimes under endogeneity,” *Journal of the American Statistical Association*, 116(533), 162–173.
- Groenwold, R. H. (2020), “Informative missingness in electronic health record systems: the curse of knowing,” *Diagnostic and prognostic research*, 4(1), 1–6.
- Hahn, P. R., Murray, J. S., and Carvalho, C. M. (2020), “Bayesian regression tree models for causal inference: Regularization, confounding, and heterogeneous effects (with discussion),” *Bayesian Analysis*, 15(3), 965–1056.

- He, D., Zhang, L., Hu, H., Gu, W.-j., Lu, X., Qiu, M. et al. (2023), “Effect of early vasopressin combined with norepinephrine on short-term mortality in septic shock: A retrospective study based on the MIMIC-IV database,” *The American Journal of Emergency Medicine*, 69, 188–194.
- He, S., Fan, C., Ma, J., Tang, C., and Chen, Y. (2022), “Platelet transfusion in patients with sepsis and thrombocytopenia: a propensity score-matched analysis using a large ICU database,” *Frontiers in Medicine*, 9, 830177.
- Hou, N., Li, M., He, L., Xie, B., Wang, L., Zhang, R. et al. (2020), “Predicting 30-days mortality for MIMIC-III patients with sepsis-3: a machine learning approach using XGboost,” *Journal of translational medicine*, 18(1), 1–14.
- James, N. D., Sydes, M. R., Clarke, N. W., Mason, M. D., Dearnaley, D. P., Spears, M. R. et al. (2016), “Addition of docetaxel, zoledronic acid, or both to first-line long-term hormone therapy in prostate cancer (STAMPEDE): survival results from an adaptive, multiarm, multistage, platform randomised controlled trial,” *The Lancet*, 387(10024), 1163–1177.
- Jiang, R., Lu, W., Song, R., and Davidian, M. (2017), “On estimation of optimal treatment regimes for maximizing t-year survival probability,” *Journal of the Royal Statistical Society Series B: Statistical Methodology*, 79(4), 1165–1185.
- Johnson, A. E., Pollard, T. J., Shen, L., Lehman, L.-w. H., Feng, M., Ghassemi, M. et al. (2016), “MIMIC-III, a freely accessible critical care database,” *Scientific data*, 3(1), 1–9.
- Jones, P. H., Davidson, M. H., Stein, E. A., Bays, H. E., McKenney, J. M., Miller, E. et al. (2003), “Comparison of the efficacy and safety of rosuvastatin versus atorvastatin, simvastatin, and pravastatin across doses (STELLAR Trial),” *The American journal of cardiology*, 92(2), 152–160.
- Karatzoglou, A., Smola, A., Hornik, K., and Zeileis, A. (2004), “kernlab – An S4 Package for Kernel Methods in R,” *Journal of Statistical Software*, 11(9), 1–20.
- Khanna, A. K., Kinoshita, T., Natarajan, A., Schwager, E., Linn, D. D., Dong, J. et al. (2023), “Association of systolic, diastolic, mean, and pulse pressure with morbidity and mortality in septic ICU patients: a nationwide observational study,” *Annals of Intensive Care*, 13(1), 1–13.

- Künzel, S. R., Sekhon, J. S., Bickel, P. J., and Yu, B. (2019), “Metalearners for estimating heterogeneous treatment effects using machine learning,” *Proceedings of the National Academy of Sciences*, 116(10), 4156–4165.
- Li, F., Ding, P., and Mealli, F. (2023), “Bayesian causal inference: a critical review,” *Philosophical Transactions of the Royal Society A*, 381(2247), 20220153.
- Li, J., Liu, H., Wang, N., Wang, F., Shang, N., Guo, S., and Wang, G. (2024), “Persistent high sepsis-induced coagulopathy and sequential organ failure assessment scores can predict the 28-day mortality of patients with sepsis: A prospective study,” *BMC Infectious Diseases*, 24(1), 282.
- Li, Z., Chen, J., Laber, E., Liu, F., and Baumgartner, R. (2023), “Optimal treatment regimes: a review and empirical comparison,” *International Statistical Review*, .
- Linero, A. R., and Yang, Y. (2018), “Bayesian regression tree ensembles that adapt to smoothness and sparsity,” *Journal of the Royal Statistical Society: Series B (Statistical Methodology)*, 80(5), 1087–1110.
- McCaffrey, D. F., Griffin, B. A., Almirall, D., Slaughter, M. E., Ramchand, R., and Burgette, L. F. (2013), “A tutorial on propensity score estimation for multiple treatments using generalized boosted models,” *Statistics in medicine*, 32(19), 3388–3414.
- McCulloch, R., Sparapani, R., Gramacy, R., Spanbauer, C., and Pratola, M. (2019), *BART: Bayesian Additive Regression Trees*. R package version 2.7.
- Meyer, D., Dimitriadou, E., Hornik, K., Weingessel, A., and Leisch, F. (2019), *e1071: Misc Functions of the Department of Statistics, Probability Theory Group (Formerly: E1071), TU Wien*. R package version 1.7-3.
- Peine, A., Hallawa, A., Bickenbach, J., Dartmann, G., Fazlic, L. B., Schmeink, A. et al. (2021), “Development and validation of a reinforcement learning algorithm to dynamically optimize mechanical ventilation in critical care,” *NPJ digital medicine*, 4(1), 32.
- Rekkas, A., Paulus, J. K., Raman, G., Wong, J. B., Steyerberg, E. W., Rijnbeek, P. R. et al. (2020), “Predictive approaches to heterogeneous treatment effects: a scoping review,” *BMC Medical Research Methodology*, 20(1), 1–12.

- Roy, A. (2023), “Nonparametric group variable selection with multivariate response for connectome-based modelling of cognitive scores,” *Journal of the Royal Statistical Society Series C: Applied Statistics*, 72(4), 872–888.
- Semenova, V., and Chernozhukov, V. (2021), “Debiased machine learning of conditional average treatment effects and other causal functions,” *The Econometrics Journal*, 24(2), 264–289.
- Shin, H., Linero, A., Audirac, M., Irene, K., Braun, D., and Antonelli, J. (2024), “Treatment Effect Heterogeneity and Importance Measures for Multivariate Continuous Treatments,” *arXiv preprint arXiv:2404.09126*, .
- Singer, M., Deutschman, C. S., Seymour, C. W., Shankar-Hari, M., Annane, D., Bauer, M. et al. (2016), “The third international consensus definitions for sepsis and septic shock (Sepsis-3),” *Jama*, 315(8), 801–810.
- Taddy, M., Gardner, M., Chen, L., and Draper, D. (2016), “A nonparametric bayesian analysis of heterogenous treatment effects in digital experimentation,” *Journal of Business & Economic Statistics*, 34(4), 661–672.
- Tibshirani, J., Athey, S., Sverdrup, E., and Wager, S. (2023), *grf: Generalized Random Forests*. R package version 2.3.0.
URL: <https://CRAN.R-project.org/package=grf>
- Ursprung, S., Mossop, H., Gallagher, F. A., Sala, E., Skells, R., Sipple, J. A. et al. (2021), “The WIRE study a phase II, multi-arm, multi-centre, non-randomised window-of-opportunity clinical trial platform using a Bayesian adaptive design for proof-of-mechanism of novel treatment strategies in operable renal cell cancer—a study protocol,” *BMC cancer*, 21, 1–11.
- van Buuren, S., and Groothuis-Oudshoorn, K. (2011), “mice: Multivariate Imputation by Chained Equations in R,” *Journal of Statistical Software*, 45(3), 1–67.
- Van Der Laan, M. J., and Rubin, D. (2006), “Targeted maximum likelihood learning,” *The International Journal of Biostatistics*, 2(1).
- Wager, S., and Athey, S. (2018), “Estimation and inference of heterogeneous treatment effects using random forests,” *Journal of the American Statistical Association*, 113(523), 1228–1242.

- Wendling, T., Jung, K., Callahan, A., Schuler, A., Shah, N. H., and Gallego, B. (2018), “Comparing methods for estimation of heterogeneous treatment effects using observational data from health care databases,” *Statistics in medicine*, 37(23), 3309–3324.
- White, W. B., Weber, M. A., Sica, D., Bakris, G. L., Perez, A., Cao, C. et al. (2011), “Effects of the angiotensin receptor blocker azilsartan medoxomil versus olmesartan and valsartan on ambulatory and clinic blood pressure in patients with stages 1 and 2 hypertension,” *Hypertension*, 57(3), 413–420.
- Williams, G., Huang, J. Z., Chen, X., Wang, Q., and Xiao, L. (2020), *wskm: Weighted k-Means Clustering*. R package version 1.4.40.
URL: <https://CRAN.R-project.org/package=wskm>
- Xu, J., Cai, H., and Zheng, X. (2023), “Timing of vasopressin initiation and mortality in patients with septic shock: analysis of the MIMIC-III and MIMIC-IV databases,” *BMC Infectious Diseases*, 23(1), 1–10.
- Xue, J., and Liang, F. (2017), “A robust model-free feature screening method for ultrahigh-dimensional data,” *Journal of Computational and Graphical Statistics*, 26(4), 803–813.
- Zeileis, A., and Grothendieck, G. (2005), “zoo: S3 Infrastructure for Regular and Irregular Time Series,” *Journal of Statistical Software*, 14(6), 1–27.
- Zhang, B., Tsiatis, A. A., Laber, E. B., and Davidian, M. (2012), “A robust method for estimating optimal treatment regimes,” *Biometrics*, 68(4), 1010–1018.
- Zhang, J., Du, L., Li, J., Li, R., Jin, X., Ren, J., Gao, Y., and Wang, X. (2022), “Association between circadian variation of heart rate and mortality among critically ill patients: a retrospective cohort study,” *BMC anesthesiology*, 22(1), 45.
- Zhu, Y., Zhang, J., Wang, G., Yao, R., Ren, C., Chen, G. et al. (2021), “Machine learning prediction models for mechanically ventilated patients: analyses of the MIMIC-III database,” *Frontiers in medicine*, 8, 662340.

Supplementary Materials for ‘Individualized
Multi-Treatment Response Curves Estimation using
RBF-net with Shared Neurons’

PETER CHANG, ARKAPRAVA ROY

Department of Biostatistics, University of Florida, United States

pchang27@ufl.edu, arkaprava.roy@ufl.edu

October 21, 2024

Figure 1: Distribution of the average residuals $\frac{1}{S} \sum_s y_{i,s} - \hat{f}_{g,s}(\mathbf{x}_i)$ obtained fitting the model, using the log-transformed length of stay in the ICU as the outcome. We generate 1000 MCMC samples from an original pool of 15000 samples, incorporating a burn-in phase of 5000 samples and thinning. These samples are then used to perform individual regressions to obtain the residuals for the s -th regression.

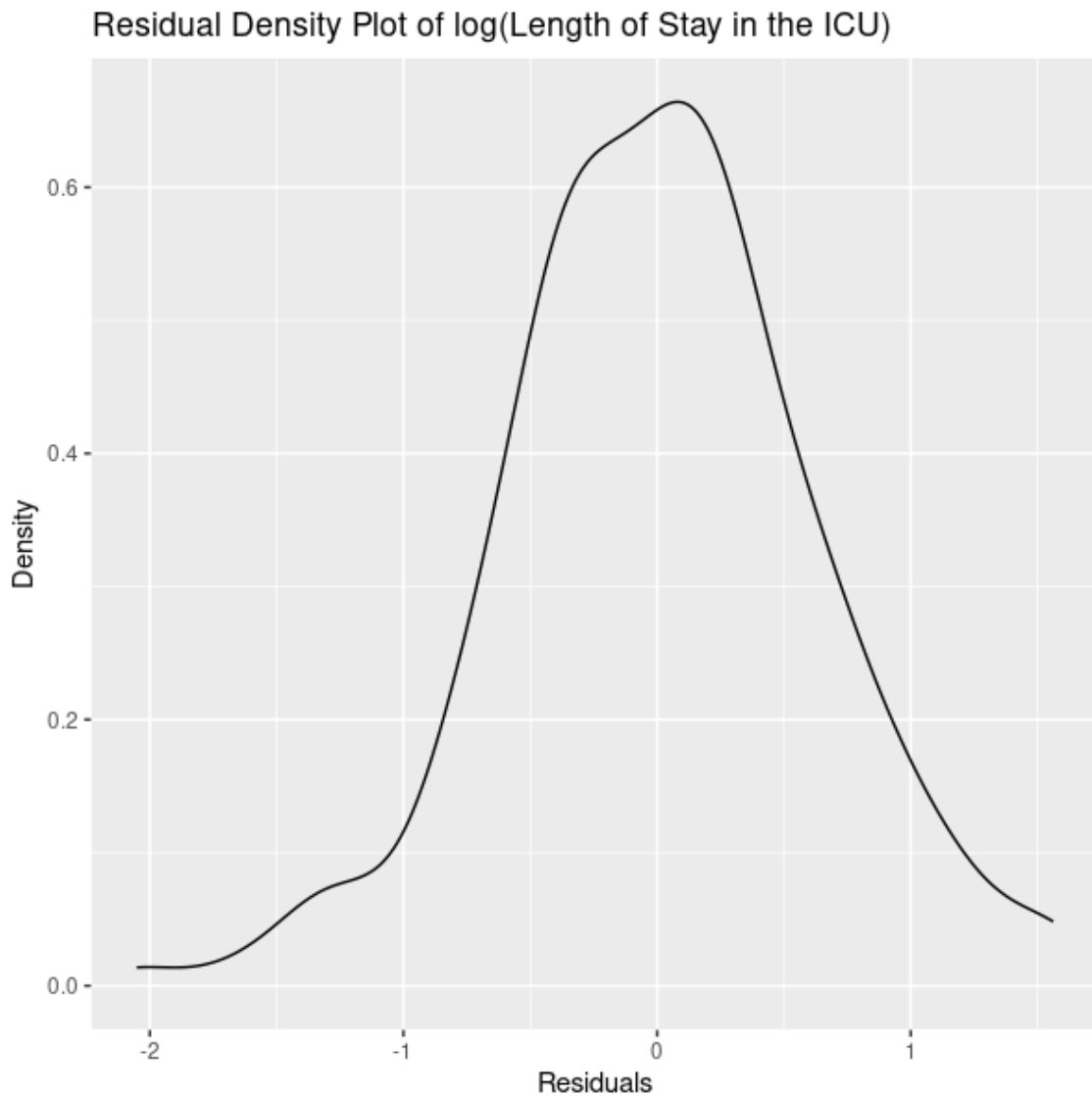


Figure 2: Distribution of the average residuals $\frac{1}{S} \sum_s y_{i,s} - \hat{f}_{g,s}(\mathbf{x}_i)$ obtained fitting the model, using the square-root transformed 12-th hour SOFA scores as the outcome. We generate 1000 MCMC samples from an original pool of 15000 samples, incorporating a burn-in phase of 5000 samples and thinning. These samples are then used to perform individual regressions to obtain the residuals for the s -th regression.

